

# Speckle observations of binary stars with a 0.5 m telescope

A. Rutkowski<sup>1</sup> & W. Waniak<sup>2</sup>

<sup>1</sup> N. Copernicus Astronomical Center, Bartycka 18, 00-716 Warsaw, Poland

<sup>2</sup> Astronomical Observatory of Jagiellonian University, Orla 171, 30-244 Cracow, Poland

the date of receipt and acceptance should be inserted later

**Abstract.** We present 36 observations of 17 visual binaries of moderate separation (range from 0.15'' to 0.79'') made with the 50 cm Cassegrain telescope of the Jagiellonian University in Cracow. The speckle interferometry technique was combined with modest optical hardware and a standard photometric CCD camera. We used broad-band V,R,I filters without a Risley prism to reduce differential colour refraction, so we performed model analysis to investigate the influence of this effect on the results of measurements. For binary components of spectral type O-F, the difference of three spectral classes between them should bias their relative positions by no more than a couple of tens of milliarcseconds (mas) for moderate zenith distances. The statistical analysis of our results confirmed this conclusion. A cross-spectrum approach was applied to resolve the quadrant ambiguity. Our separations have RMS deviations of 0.012'' and our position angles have RMS deviations of 1.8°. Relative photometry in V, R and I filters appeared to be the less accurately determined parameter. We discuss our errors in detail and compare them to other speckle data. This comparison clearly shows the high value of our measurements. We also present an example of the enhancement of image resolution for an extended object of angular size greater than the atmospheric coherence patch using speckle interferometry techniques.

**Key words.** Binaries: visual - Techniques: interferometric - Techniques: high angular resolution - Astrometry

## 1. Introduction

Although during the last decade adaptive optics has pushed the once prominent technique of speckle interferometry (Labeyrie 1970) into the background, this method still provides a simple, inexpensive tool for determination of the orbital and photometric parameters of visual binary stars in the course of surveys made with small and moderate sized telescopes. Many such projects have been completed in the last years (e.g. Mason et al. 2004a, 2004b, Prieur et al. 2003, Scardia et al. 2005). Substantial technical and programming improvements, as well as the widespread use of CCD cameras among small observatories and amateurs, make it possible to perform both speckle observations of binary stars (with quite good precision) and also diffraction-limited speckle imaging of compact extended objects.

In this paper, we show how a standard photometric CCD camera usually used for broad-band photometry of variable stars and comets, can be inexpensively modified into an uncomplicated "specklegraph", which can supply measurements of binaries hardly inferior to the results of observations with a 1-m class telescope equipped with classical speckle cameras which include reducers of differential colour refraction and/or narrow-band filters. For the trial run we selected a number

of binary stars with separations ranged from one half of the diffraction limit of the telescope for visible light up to 1'' and brighter than about 8 mag in V. Some of them have relatively precise orbital parameters (e.g. WDS15232+3017), some have extremely inaccurate orbits (e.g. WDS11137+2008), whereas others are still waiting for such a determination.

In the following paragraphs we describe our equipment, observational procedure and the reduction method of speckle images. Before presenting our results we discuss the problem of the influence of differential colour refraction. Conclusions reached from model computations are confronted with the observations. We present orbital O-C analyses for pairs with well known orbits. We also show an example of how the image resolution degraded by seeing can be improved for extended objects with angular dimensions greater than the radius of the atmospheric coherence patch.

## 2. Equipment

The observations were performed using a Cassegrain telescope (0.5 m diameter and 6.7 m focal length), with a PHOTOMETRICS S300 CCD camera with a SI003B thinned, back-illuminated chip manufactured by SITe. It has 1024x1024 square pixels of the side 24  $\mu\text{m}$  and a 16 bit A/D converter. The camera works in the Multi Pinned Phase (MPP) mode with a

thermoelectric+liquid cooling system, which maintains operating temperature close to  $-50^{\circ}\text{C}$ .

We observed with the set of standard V,R,I filters specially designed for CCD (Bessell 1990) manufactured by CUSTOM SCIENTIFIC. U and B filters were not used for two reasons. The first was the diminishing of the useful signal due to relatively low quantum efficiency of the CCD in this range and atmospheric extinction. The second was the possibly high bias of the measured positions of the binary components by differential colour refraction. Model analysis of this effect confirmed our approach.

The typical angular scale of the chip, equal to 0.736 arcsec/pixel, is insufficient for proper sampling of a specklegram, so we used a projector giving appropriate enlargement. This has the form of a duralumin tube of length 150 mm and inner diameter 40 mm, attached to the back side of the filter wheel chassis. The CCD camera is mounted to the back flange of this tube. The optimised connecting system assures straightforward and quick (up to a minute) installation of the projector. Great attention was paid to the removing rotational backlash. Inside the tube, typical microscope objectives (10x or 20x) can be mounted interchangeably.

The angular scale of our "speckle camera" for the 10x objective was obtained from astrometry of  $\alpha$  Gem (Castor, WDS07346+3153=ADS 6175) and relative positions from Hipparcos data. Separation of the components (close to  $4''$ ) exceeding separations of our target pairs and close proximity of spectral classes (A1V, A2V) minimising differential colour refraction make this object highly suitable for astrometric calibration. In the case of the 20x objective we used combined results from speckle interferometry of Castor and WDS15232+3017=ADS9617. The latter star has precisely obtained orbital parameters (grad 1), and is recommended as an astrometric calibrator by Hartkopf & Mason (2003a). The scales of our frames were equal to  $0.0824 \pm 0.0002$  and  $0.04760 \pm 0.0007$  arcsec/pix for the 10x and 20x objectives, respectively. The precision of determination of position angle was close to  $0.1^{\circ}$ . This error was the result of a small rotational backlash in the focusing head to which the whole assembly of the filter wheel, the projector and the camera was mounted. We did not notice any serious image deformations which could be given by the projector.

As our CCD camera is typically dedicated to precise photometry it has low Read Out Noise (RON) but relatively long read-out time of 13 sec per frame. Taking into account the precision of our autoguider system and the relatively bad seeing (frequently exceeding  $3''$ ) we decided to use a sub-frame of  $256 \times 256$  pixels, where the readout time was close to 2 sec. Comparing the readout frequencies of typical speckle cameras (tens of cycles per second) with our system it is obvious that our observations have low efficiency. On the other hand they ensure full statistical independence of consecutive frames for larger and longer-lasting wave-front disturbances. An attempt to use the promising drift scanning mode (Fors et al. 2001) enhanced our speed only by a factor of two while producing prominent streaking between speckle images. In the end we used the common mode of data transfer.

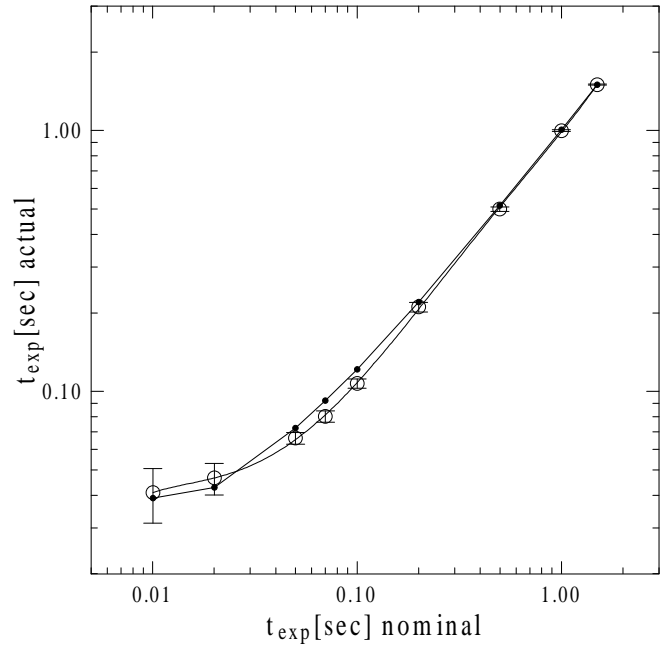


**Fig. 1.** Dependence between actual (achieved) and nominal (set by the observer) exposure times for the iris shutter of the CCD camera. Thin solid line: 5th order polynomial fit to the data. Thick solid line with dots: simple mechanical model of the shutter.

Of crucial importance for the proper realisation of speckle interferometry is the fulfilment of the condition of frozen turbulence. This means using extremely short exposure times (of the order of milliseconds). Our electronically controlled iris shutter has a nominal exposure time of up to 1 msec, but its dead time is of the order of 50 msec. Therefore, we were forced to determine actual achieved exposure times and investigate their repeatability. We obtained images of a bright star using nominal exposure from 2 sec (where the dead-time effect is invisible) up to 10 msec. The results are presented in Fig. 1. The conclusion is that the shortest achievable integration time is close to 40 msec, quite comparable with the dead-time of the shutter. Analysis of the dependence observed in this figure using a simple model which included the mechanical inertia of the shutter showed that the magnetic hysteresis of the electromagnet should be taken into account.

### 3. Observations and reductions

Speckle observations were performed during 13 nights from March to June 2003. Almost all binary stars satisfying the conditions described in the first paragraph and visible at the appropriate conditions during this period were studied. We tried to observe as large fraction of our sample as possible with different PSF standards, filters and exposure times to get a feeling of how the obtained parameters depend on them.

A typical observing run consists of a series of 100 dark frames, 300 frames of a PSF standard (one half obtained before, and one half after the observation of the binary) and 300 frames of the object of interest. We realised two to three such series

for each star per night. The duration of a single run was shorter than about half an hour, which ensured limited variation of the seeing conditions.

Flat frames were obtained on the twilight sky using exposure times the same as were used for observing the binaries. This was extremely important for taking into account the non uniform illumination of the field of view given by the iris shutter for extremely short exposures. PSF standards were chosen as close on the sky to the binary stars as possible, considering the zenith distances and the spectral classes. Nominal exposure times ranged from 10 to 100 msec, which means that achieved integration times were from 40 to 107 msec. Generally, we correlated them with the brightness of the binary and PSF standard and the separation of the components. Shorter exposures imply better contrast of the speckle structure but a lower signal level. Anticipating discussion of the results, we can ascertain that using different integration times we obtained astrometry of the same class of precision.

We started the data reduction with subtraction of the mean dark frame, which for such short expositions mainly carries information about the bias level. After flat-fielding of the object frames, we shifted the images of the speckle patterns to the central position on the frame, to facilitate later steps of the data processing. Substantial chaotic transitions of the pattern were produced both by wave front tilts and autoguiding process, which had an overall precision of  $1''$ . Next we conducted apodization of the frames with a smooth circular mask. The unmasked region had a diameter large enough to encircle the whole visible speckle pattern while small enough to cut off as much of the noisy surroundings as possible.

After computing the mean Fourier power spectra of the images of both binary stars and PSF standards, we subtracted from them the mean power spectrum of the dark frames apodized by the appropriate mask as well as photon noise bias (Dainty & Greenaway 1979) estimated by the mean level of the spectra beyond the diffraction limit. At this stage of the data reduction process we compared the spectra of the PSF specklegrams observed before and after the binary. In the case of full agreement between them we combined both results into one set, which was reanalysed to give the final power spectrum of the standard. The spectrum of the binary was then divided by the PSF spectrum treated as a Wiener filter (Keller & Johannesson 1995). The distance between binary components, the position angle and the relative brightness were obtained from LSQ fitting of a sinusoid to the resultant power spectrum. We masked the central part, where the seeing peak dominates, and the outside regions, where the S/N ratio is too low a the cut-off of spatial frequencies greater than the diffraction limit takes place. No other weighting of the input data was applied. After close inspection of the images we discarded the classical  $\chi^2$  approach (Horch et al. 1997) as the photon and read-out noise were not only source of the variance seen in the power spectra. Quasi-systematic horizontal noisy structures played a quite serious role in our dark frames. They produced weak vertical structures in the images of the power spectrum, structures which were only partially removed by the subtraction procedure.

To resolve the quadrant ambiguity, we used the cross-spectrum approach by Knox & Thompson (1974) (see also

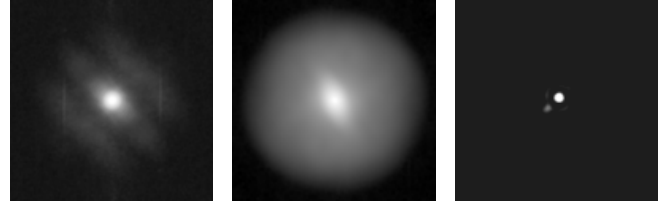


**Fig. 2.** Example of speckle imaging for WDS 04100+8042=ADS 2963. Left panel: raw spectrum of the binary, middle panel: spectrum of the PSF standard, right panel: image reconstructed by cross-spectrum analysis. Separation between components is 0.78 arcsec. North is up and East is to the left.

Christou 1991) analysing 8 sub-plains computed for 8 shifts from a given pixel towards all its neighbour. The resultant frame bearing phase information was obtained by an iterative LSQ approach. In the case when the distance between binary components was greater than the diffraction limit, we were able to obtain two separate peaks. For closer components the asymmetry of the elongated profile of three overlapped peaks (one central and two satellites) made it possible to resolve the quadrant ambiguity. An example of the result of our speckle imaging procedure for the binary star WDS 04100+8042=ADS 2963 is presented in Fig. 2.

#### 4. Theoretical differential colour refraction

Prior to presenting the results of our speckle interferometry, we must discuss in detail the effect of differential colour refraction (DCR). As our observations were performed without a Risley prism corrector and with broad-band V,R,I filters we must pay great attention to this phenomenon.

The dependence of colour refraction on the atmospheric temperature, pressure and relative humidity as well as spectral classes of stars (taking into account broad-band photometry systems) has been investigated both theoretically and observationally (e.g. Stone 1996, 2002, Gubler & Tytler 1998, Mal'yu to & Meinel 2000, Langhans et al. 2003). Computing the DCR effect we used formulae for atmospheric refraction taken from Stone (1996). The only modification was the replacement of the spectral energy distribution of the star by the spectral distribution of the number of photons, which is suitable for quantum sensitive detectors such as CCDs. We used the dependence of the quantum efficiency upon wavelength and the transmittance curves of our filters as given by the manufacturers. The transmission of the atmosphere was reconstructed from the mean extinction coefficients in the U,B,V,R,I bands (Siwak, private communication), taking into account the absorption by ozone and both Rayleigh and aerosol scattering. We assumed the transmittance of interstellar matter characteristic for the colour excess  $E(B-V)=0.3$ , although we examined the DCR effect for other values. We used the spectral energy distributions for appropriate spectral classes taken from the BaSeL Stellar Library (<http://www.astro.mat.uc.pt/BaSeL>) compiled by Lejeune et al. (1998). We considered two luminosity classes (dwarfs and giants) assuming only solar metallic-

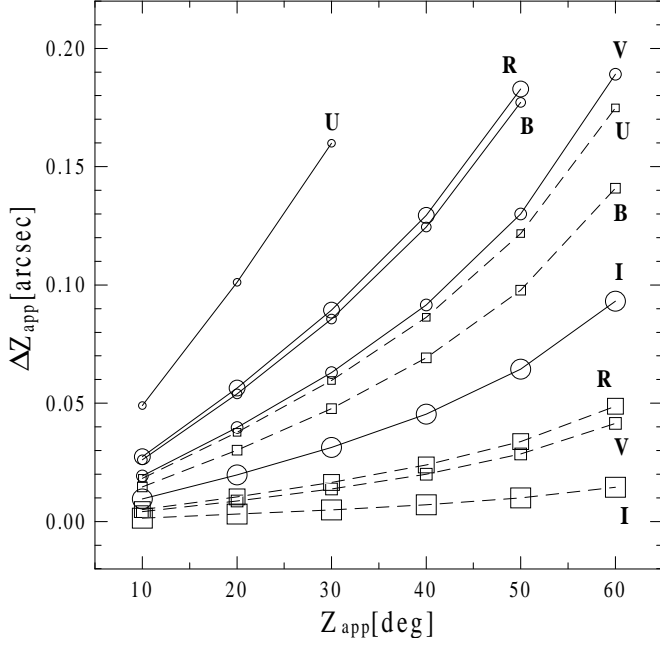


**Fig. 3.** Atmospheric differential colour refraction versus apparent zenith distance of a pair of dwarf stars with a Solar value of  $\text{Log}(g)$ . Open circles connected by solid line: effect for binary star composed of O5 and M5 components. Open squares connected by dashed line: binary star with O5 and F5 stars.

ity. The sensitivity of the results on the last parameter appeared to be negligible.

As the first step, we investigated the dependence of the DCR phenomenon on the ground-level temperature, pressure and relative humidity for the values characteristic for our observatory. As could be expected, taking into account previous results (e.g. Malyuto & Meinel 2000), the correlation between the effect and these parameters is negligible. Therefore, in further computations we used standard atmospheric temperature and pressure assuming 60% humidity, which is typical for our location in spring and early summer. The first task was to check how the differential refraction depends on the difference in the zenith distances of the binary components. It appeared that for a  $1''$  difference for all spectral classes and all filters this effect is of the order of  $0.001''$ , if observations are made at  $60^\circ$  zenith distance.

Taking into account the precision of our determination of the astrometric parameters, we assumed further on that both components were at an identical zenith distance.

Of the various results which we obtained, only the most important are presented here. Fig. 3 shows the dependence of the DCR effect on the zenith distance of the binary star for two cases of the difference between spectral types and for all filters which we were able to use. This result fully confirms our decision to use only V,R,I filters in our observations. Although the O5-M5 difference between components makes it impossible to obtain reasonable astrometric results, the interval of three classes gives an effect less than  $0.02''$  for a zenith distance smaller than  $40^\circ$  for all three filters used. As could be expected for the I filter the DCR effect is the smallest (less than

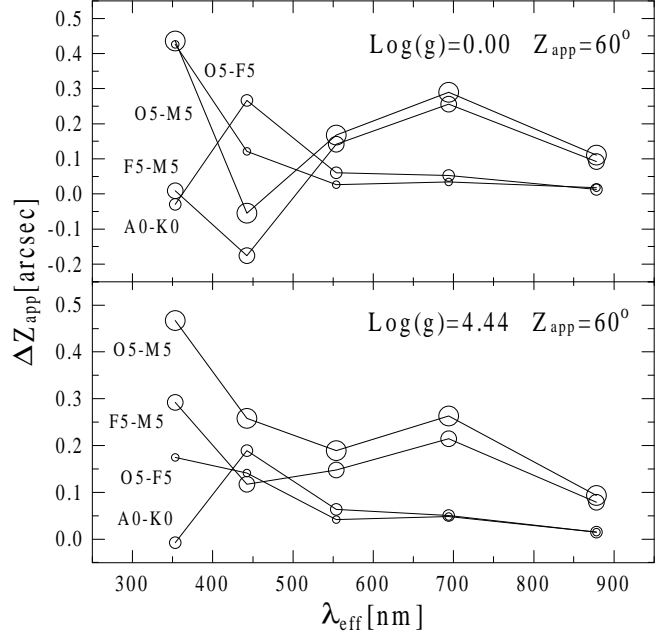


**Fig. 4.** Atmospheric differential colour refraction for UBVR filters for an apparent zenith distance of  $60^\circ$  and two luminosity classes. The X-axis gives the effective wavelength of the filters. Four different cases of spectral classes of the components of the binary star are presented.

$0.01''$  for  $z < 50^\circ$ ). The R filter gives the worst results, due to the fact, that the effective width of its spectral profile is about twice the width of the profile of the V filter.

Fig. 4 presents the DCR effect at  $60^\circ$  zenith distance versus the effective wavelength of the filter for two luminosity classes of the binary components (a pair of dwarfs and a pair of giants) and for various differences of the spectral types of the components. The results for the pair dwarf+giant is not so different as to need to be presented. As can be seen, the sequence of the filters ordered according to increasing DCR effect (I,V,R) generally does not depend on the spectral or luminosity class. A smaller effect for these three filters can be expected for earlier spectral types. A late spectrum implies a more complex spectral energy distribution in the long wavelength range. The DCR effect for the U,B filters appears to depend on the spectral and luminosity classes in quite a complicated way. This is once another argument against observing through the broad-band short wavelength filters.

Surprisingly, cases exist for which the effect for the least suitable U filter is smaller than for B filter and of the order of the effect for the V,R,I filters. It occurs for moderate spectral classes where the Balmer jump makes the effective spectral profile of the U filter when combined with stellar spectrum relatively narrow.

## 5. Results and discussion

Table 1 presents the results of our speckle interferometry. It gives separations, position angles and magnitude differences between components for the observation moments expressed

in Besselian years. In cases when more than one observation of a given binary was performed during a night the results were averaged and the mean values were put under horizontal line. Errors of the parameters were derived from LSQ fitting of a sinusoid to the mean power spectrum of the specklegrams. They include the errors of determination of the scale and position angle of our frames. It is not surprising that the discrepancies of the parameters obtained from the LSQ approach are rather underestimated due to the correlations between the parameters themselves. Only for multiple observations can appropriate values of the errors be received. Errors of the mean values of the parameters presented in Table 1 merge the two kinds of cited above. To give a feeling of how high the real errors of the astrometric parameters could be in cases when only a single observation of the binary star was made, we compared errors the given by LSQ fitting with the errors obtained from multiple observations. The correlations were quite good and show that the real error of the separation should be about 3 times and the error of the position angle about 4 times greater than the formal LSQ error.

Even superficial inspection of Table 1 shows that the astrometric results are almost independent of filter, exposure time and PSF standard used, especially taking into account the precision of our measurements. On the other hand, magnitude differences show serious discrepancies, particularly if the separation of the components becomes comparable or smaller than our diffraction limit. This is fully understandable in the case of LSQ fitting. Thus, only consistent multiple results of the determination of the magnitude difference for the separation of a pair larger than diffraction limit can give reliable information (WDS04100+8042=ADS2963, WDS14139+2906=ADS9174, WDS18208+7120=ADS11311). The remaining results should be treated only as rough approximations.

To investigate statistically the possible biasing of our astrometric results by the DCR effect, we analysed differences between the actual and the mean relative positions of the components for multiple measurements. They were referred to a horizontal-vertical reference system. The DCR effect should be manifested for the vertical component of the dispersion since the consecutive measurements were performed at different zenith distances. Fig. 5 shows these discrepancies separated into two classes. For V,R filters (first group) the effect should be on average greater than for the I filter (second group). As one can see, the difference between vertical and horizontal dispersions is slightly significant and any correlation between the magnitude of the effect and the filter could be discern. The conclusion is that from the statistical point of view our observational conditions and the differences between the spectral/luminosity classes of the components were on average very favourable, producing negligible DCR effect.

Fig. 6 presents the uncertainties of  $\rho$  and  $\theta$  (defined as previously but referred to the polar reference system) versus the separation of the components. The only trend is an increase of  $\Delta\theta$  with decreasing  $\rho$ , which is quite normal. The RMS values of the discrepancies are  $0.012''$  for  $\rho$  and  $1.8^\circ$  for  $\theta$ . If one wants to consider results obtained for the separations larger than, or at least close to, the diffraction limit one should reject star WDS22330+6955=16057. Then, the mean dispersion

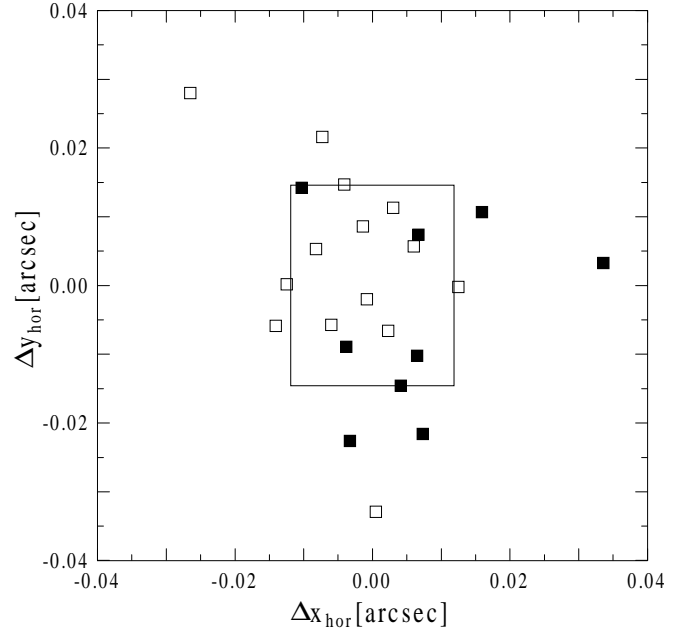


**Fig. 5.** Dispersion of the observational points in the rectangular horizontal-vertical coordinate system. The Y - axis is parallel to the vertical coordinate and measures dispersion of the zenith distances. The figure presents (O-C) differences between the mean (for at least two measurements) and actual for a given star. The central rectangle shows  $1\sigma$  bands for x and y at 0.012 and 0.015 arcsec respectively. Open squares are for V,R filters and filled symbols represent the I filter.

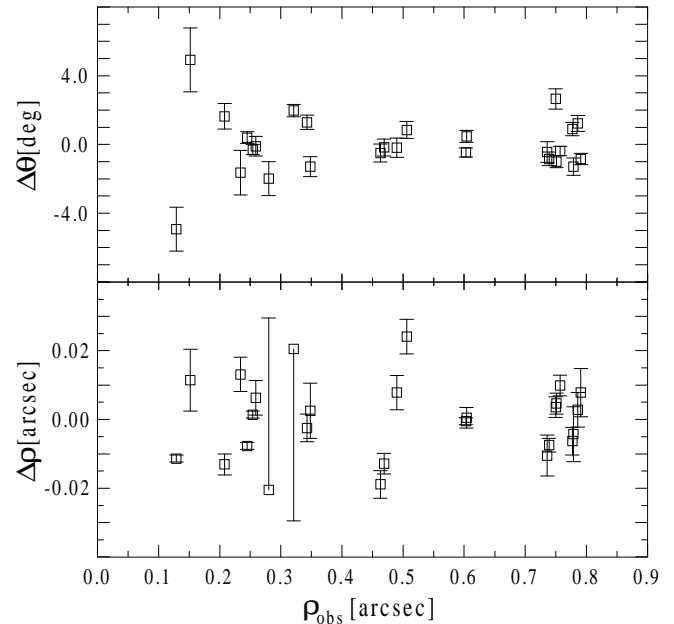


**Fig. 6.** Dispersion of the position angles and angular separations as a function of the separation between components. This figure presents  $(O - C)_\rho$  and  $(O - C)_\theta$  differences between the mean (for at least two measurements) and actual values for a given star. The error bars were inferred from the LSQ fitting procedure of the speckle power spectrum.

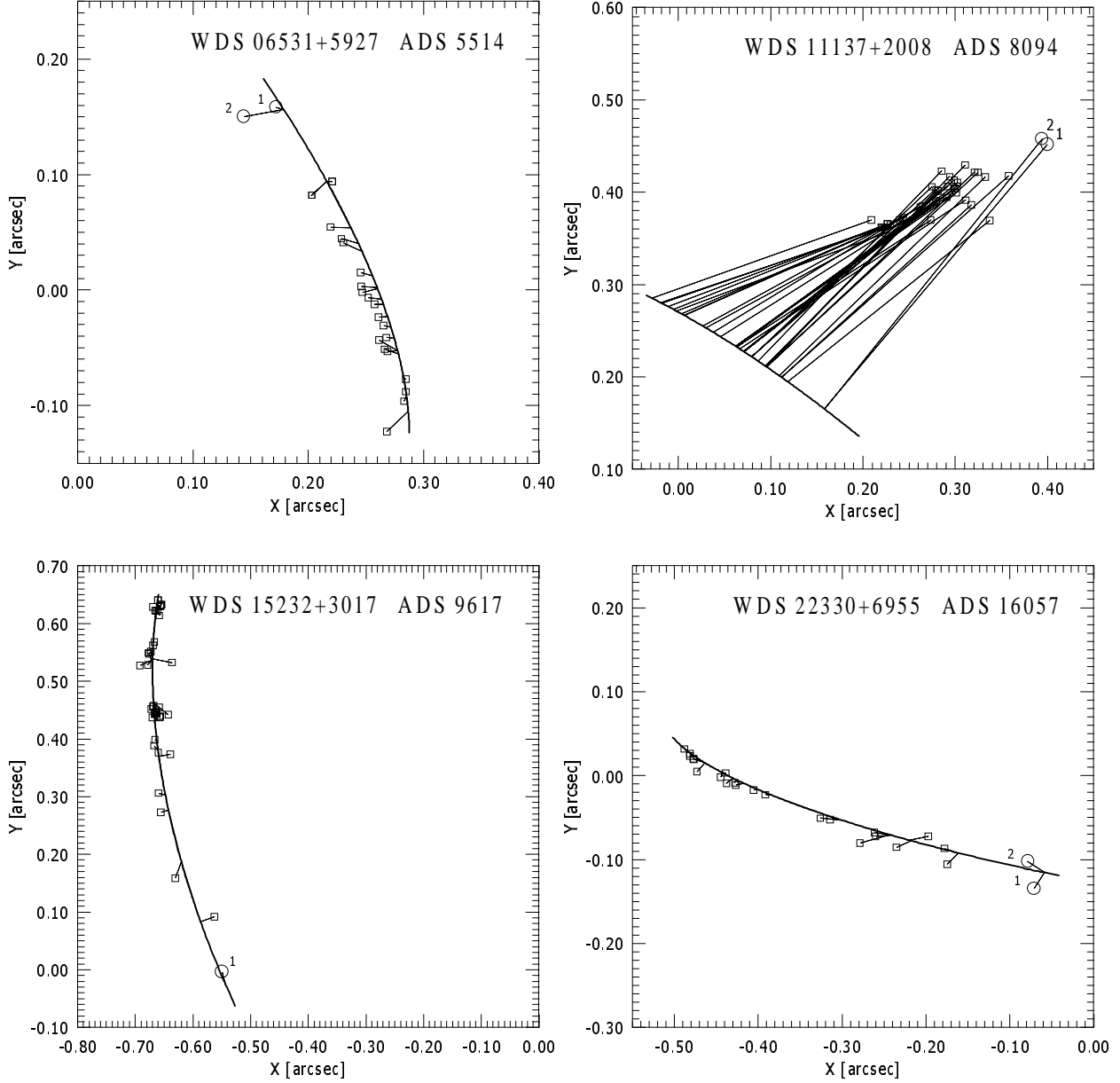


**Fig. 7.** Comparison of our astrometric results (open circles) with other speckle interferometric results compiled in Hartkopf et al. (2004) (open squares) and actual orbits according to the orbital elements listed in the 6-th Catalog of Orbits of Visual Binary Stars (Hartkopf & Mason 2003a). Line segments are drawn from the measured positions to the ephemeris points. North is up and East is to the left.

of the separation is almost unchanged, whereas the mean dispersion of  $\theta$  drops to  $1.2^\circ$ . The precision of our measurements is comparable to typical values for 1 m class telescopes. Fors et al. (2004) using a 1.5 m telescope presented an accuracy of  $0.017''$  and  $1.5^\circ$  respectively. Measurements by Scardia et al. (2005) made with the PISCO instrument (Priour et al. 1998) moved to Merate and attached to 1 m telescope had an overall dispersion of about  $0.01''$ .

To compare our position angles and separation measures with the results of other observers and with ephemerides we took the observational data compiled in the Fourth Catalog of Interferometric Measurements of Binary Stars (Hartkopf et al.

2004) and actual orbital elements in the 6th Catalogue of Orbits of Visual Binary Stars (Hartkopf & Masnon 2003a). Fig. 7 presents such comparisons for 4 selected pairs having different grades of orbit determination. An especially odd case is WDS1137+2008=ADS8094, for which it seems that the "orbital" motion is a typical proper motion of two separate stars.

To give general information of how good our results are, compared to other results of speckle interferometry, we should not only analyse the differences between the ephemeris positions and ours, but compare these differences with the total behaviour of the O-C measure. A spectacular example, which supports our approach, is WDS1137+2008=ADS8094 (men-

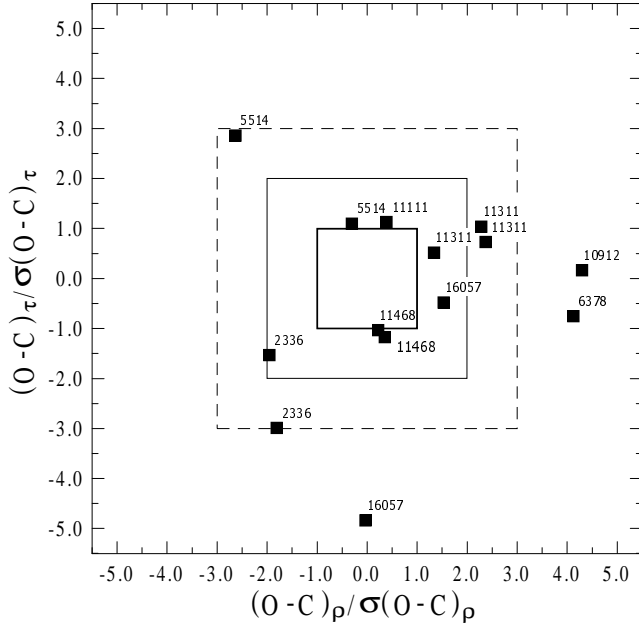


**Fig. 8.** Relative (O-C) for a number of stars presented in the coordinate system of angular separation  $\rho$  and tangential displacement  $\tau = \rho(O - C)_\theta$ . This plot shows ratios of the actual (O-C) values to the RMS of (O-C) inferred from speckle results compiled in Hartkopf et al. (2004) and actual orbits taken from the 6-th Catalog of Orbits of Visual Binary Stars (Hartkopf & Mason 2003a). Thick, thin and dashed lined squares mark 1, 2 and  $3\sigma$  boxes respectively. The binaries are described by ADS numbers.

tioned above). Thus, for our binary stars having orbits of grade better or equal to 4 and which do not exhibit systematic temporal trends of the O-C measure, we computed our differences between observed and ephemeris positions and divided them by the RMS averaged O-C values for all the results cited in Hartkopf et al. (2004). Fig. 8 presents our relative O-C discrepancies and 1, 2, 3  $\sigma$  boxes. Although none of the points fit inside the  $1\sigma$  square, only 3 measurements of 14 are outside the  $3\sigma$  box. Examining this result one should bear in mind that a considerable fraction of the observations presented in Hartkopf et al. (2004) were performed with a few meters class telescopes and with correctors of the DCR effect. As can be seen from Fig. 8 no substantial bias in the angular separation or in the position angle exists in our data.

We also averaged direct O-C measures and computed their RMS values for the group of binary stars described above but without WDS22330+6955=16057, for which the angular separation is below the diffraction limit. For the position angle we obtained a mean O-C value equal to  $-0.40^\circ$  and the RMS of  $2.89^\circ$ . In the case of the separation, these values were  $0.010''$  and  $0.046''$ , respectively. Our O-C measures for a number of stars can be directly compared to the most recent results received by Mason et al. (2004a, 2004b) with 0.66 m USNO refractor. On average our values of the discrepancies between observed and ephemeris positions are close to the discrepancies given by Mason.

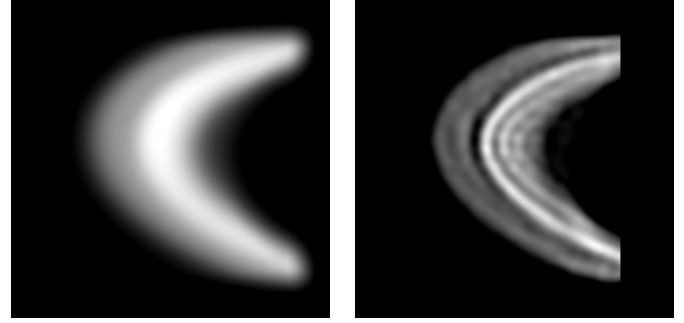


**Fig. 9.** Example of using speckle interferometry with the cross-spectrum technique to enhance image resolution in the case of an extended object larger than the atmospheric coherence patch. The figure presents a fragment of Saturn's rings with the disk of the planet masked. Left panel: usual 15 sec exposure, right panel: image reconstructed from 300 speckle images. The side of the frame has 20 arcsec. North is up and East is to the left.

As a by-product of our speckle interferometry we obtained the speckle frames of bright extended objects, such as Saturn, Io, and Ganymede. Here we present the results of speckle image reconstruction of a fragment of Saturn's rings as an example of the enhancement of resolution degraded by seeing. At the beginning we observed the entire ring structure using  $512 \times 512$  frames instead of  $265 \times 265$  and attempted to reconstruct the image, but the result was only slightly better than the usual image degraded by seeing. Therefore, we omit this discussion here. During the night of 27 March 2003, we obtained 300 specklegrams of a half of the full ring with 0.05 sec nominal exposure time, using the I filter and 10x microscope objective. As a PSF standard we used BS1910. The problem of crucial importance during the data reduction was to properly apodize the speckle frames. First, we prepared the mask, which removed half of the planetary disk and apodized the borders of the image with a cosine function. Before masking, all the frames were shifted to overlap one another using the cross-correlation method. After computing the mean power spectrum of the apodized specklegrams we proceeded in the same way as for binary stars. Fig. 9 shows the reconstructed image (right panel) compared with the usual exposition obtained during the same night for  $2''$  seeing (left panel). The size of the frame is 20 arcsec, which is at least a few times greater than the average radius of the atmospheric coherence patch. In this case a partial reduction of the seeing effect was obtained but the image resolution was substantially enhanced. An additional effect is a distinct, though not strong excessive deconvolution of the ring structure, manifesting itself by too high contrast between the rings and divisions and knotty artefacts visible in the image. Nevertheless, the bright A,B rings as well as Encke and Cassini divisions are quite clearly visible.

## 6. Conclusions

We have presented the results of the first speckle interferometry observations of visual binary stars made with the 50 cm

Cassegrain telescope of the Jagiellonian University in Cracow. By adding a simple image projector with a microscope objective to the standard solution for the broad-band CCD photometry, we obtained good spatial sampling of the frame. Using standard V,R,I filters without a DCR effect reducer forced us to perform a theoretical analysis of the influence of this phenomenon on the astrometric parameters. Statistical analysis of our observational data confirmed the model results. For V,R,I filters the DCR effect for moderate zenith distances was almost negligible, compared to the precision of our astrometry, which was about  $0.014''$  taking into account both separation and position angle measures. Such a value of the dispersion is rather typical for 1 m class telescopes if one uses LSQ fitting of the mean power spectrum by a sinusoid function. In evaluating our precision, one should bear in mind that we used a limited number of speckle images (typically 300 in one trial) and exposure times longer than 0.04 sec.

Our approach to the problem of the reconstruction of the phase information based on iterative LSQ analysis of the 8 sub-planes of the cross-spectrum gave good results, not only resolving the quadrant ambiguity but allowing us to retrieve almost diffraction limited images of the extended objects. As an example an image of a fragment of Saturn's rings was presented.

The analysis of the O-C measures of our data shows general agreement with the results of other projects observing binaries by speckle interferometry. Although our telescope is one of the smallest used for such a task, our results are hardly inferior to the results obtained with better equipped 1 m class telescopes. Thus, our ability to perform reasonable astrometry are quite promising. Unfortunately, the precision of our relative photometry of binary components were rather poor (the order of a few tens of magnitude) and requires some improvements in the data reduction.

From our results for WDS1137+2008=ADS8094, which has orbital parameters of the worst grade (Hartkopf & Mason 2003a), it is rather obvious that the relative trajectory observed until now contradicts the presumed double nature of this object.

*Acknowledgements.* We would like to thank M. Siwak for kindly supplying extinction coefficients for Cracow in the U,B,V,R,I filters.

## References

- Bessel, M.S. 1990, PASP, 102, 1181  
 Christou, J.C. 1991, ExA, 2, 27  
 Dainty, J.C. & Greenaway, A.H. 1979, J.Opt.Soc.Am., 69, 786  
 Gubler, J. & Tytler, D. 1998, PASP, 110, 738  
 Hartkopf, W.I. & Mason, B.D. 2003a, Sixth Catalog of Orbits of Visual Binary Stars., United States Naval Observatory, Washington, USA (available at <http://ad.usno.navy.mil/wds/orb6.html>)  
 Hartkopf, W. I. & Mason, B. D. 2003b, Sixth Catalog of Orbits of Visual Binary Stars. Calibration Candidates, United States Naval Observatory, Washington, USA (available at <http://ad.usno.navy.mil/wds/orb6/orb6c.html>)  
 Hartkopf, W.I., Mason, B.D., Wycoff, et al. 2004, Fourth Catalog of Interferometric Measurements of Binary Stars, United States Naval Observatory, Washington, USA (available at <http://ad.usno.navy.mil/wds/int4.html>)  
 Horch, E. P., Ninkov, Z. & Slawson, R. W. 1997, AJ, 114, 2117  
 Fors, O., Núñez, J. & Richichi, A. 2001, A&A, 378, 1100  
 Fors, O., Horch, E.P., Núñez, J. 2004, A&A, 420, 397  
 Keller, C.U. & Johannesson, A. 1995, A&AS, 110, 565  
 Knox, K.T. & Thompson, B.J. 1974, ApJ, 193, L45  
 Labyrie, A. 1970, A&A, 6, 85  
 Langhans, R., Malyuto, V. & Potthoff, H. 2003 AN, 324, 454  
 Lejeune, T., Cuisinier, F. & Buser, R. 1998, A&AS, 130, 65  
 Malyuto, V. & Meinel, M. 2000, A&AS, 142, 457  
 Mason, B.D., Hartkopf, W.I., Wycoff, G.L. et al. 2004a, AJ, 127, 539  
 Mason, B.D., Hartkopf, W.I., Wycoff, G.L. et al. 2004b, AJ, 128, 3112  
 Prieur, J.-L., Koechlin, L. André, C. et al. 1998, ExA, 8, 297  
 Prieur, J.-L., Carquillat, J.-M., Ginestet, N. et al. 2003, ApJS, 144, 263  
 Scardia, M. Prieur, J.-L., Sala, M. et al. 2005, MNRAS, 357, 1255  
 Stone, R.C. 1996, PASP, 108, 1051  
 Stone, R.C. 2002, PASP, 114, 1070



**Table 1.** Results of speckle interferometry for binary stars. Consecutive columns give: WDS and ADS numbers; fraction of the Besselian Year; nominal exposure time in msec, filter used, BS or SAO (in italics) number of the PSF standard; angular separation in arcsec together with the error and (O-C) value; position angle in deg measured from North towards East for the 2000.0 epoch, error and (O-C) value for the position angle, grade of the orbital elements (G) according to the 6-th Catalog of Orbits of Visual Binary Stars (Hartkopf & Mason 2003a), magnitude difference between components ( $\Delta$ ) together with its error and the number (N) of the note concerning the observational conditions.

WDS	ADS	2003+	$t_{\text{exp}}^{\text{nom}}$	F	PSF	$\rho$	err $\rho$	(O-C) $\rho$	$\theta$	err $\theta$	(O-C) $\theta$	G	$\Delta$	Err $\Delta$	N
03054+2515	2336	0.2327	50	V	905	0.343	0.004	-0.067	251.97	0.41	-2.78	3	0.34	0.09	1
		0.2355	70	R	905	0.348	0.008	-0.062	249.38	0.58	-5.38	3	0.55	0.12	2
04100+8042	2963	0.2334	20	I	1317	0.786	0.005	—	133.39	0.47	—	—	1.48	0.03	1
		0.2335	70	I	1317	0.777	0.004	—	133.06	0.39	—	—	1.17	0.03	1
		0.2335				0.782	0.006	0.063	133.23	0.35	-3.50	3	1.33	0.16	
		0.2418	20	R	1317	0.791	0.007	—	131.34	0.33	—	—	1.16	0.03	—
		0.2420	70	R	1317	0.779	0.008	—	130.89	0.50	—	—	1.25	0.03	—
		0.2419				0.785	0.008	0.067	131.12	0.37	-5.62	3	1.21	0.05	
05056+2304	—	0.2329	100	I	1620	0.363	0.004	—	151.16	0.71	—	—	1.34	0.02	1
06145+1754	—	0.2221	50	I	2200	0.370	0.002	—	138.17	0.44	—	—	0.43	0.05	3
06531+5927	5514	0.2062	50	I	2477	0.234	0.005	-0.003	312.67	1.30	1.69	3	1.62	0.03	4
		0.2823	20	R	2477	0.208	0.003	-0.030	316.16	0.74	4.96	3	0.69	0.04	5
07346+3153	6175	0.1816	50	R	2990	4.177	0.049	—	61.14	0.69	—	—	1.21	0.13	6
		0.1816	70	I	2990	3.987	0.600	—	61.38	0.50	—	—	1.56	0.05	6
		0.1816				4.082	0.316	-0.039	61.26	0.44	-0.73	3			
07486+2308	6378	0.2359	50	V	2951	0.321	0.050	—	37.60	0.36	—	—	0.30	0.13	2
		0.2358	50	I	2951	0.280	0.050	—	33.64	0.99	—	—	2.01	0.03	2
		0.2359				0.301	0.041	0.026	35.62	2.05	-1.18	4			
08198+0357	—	0.2879	100	R	<i>116582</i>	0.269	0.016	—	61.18	0.64	—	—	0.77	0.29	7
11137+2008	8094	0.2880	70	R	4357	0.603	0.001	0.374	318.48	0.26	2.21	5	0.43	0.03	7
		0.3373	70	I	4300	0.604	0.003	0.375	319.29	0.35	3.14	5	0.97	0.03	8
11363+2747	8231	0.1791	50	R	4357	0.750	0.003	—	148.79	0.59	—	—	1.19	0.02	—
		0.1792	50	I	4357	0.751	0.003	—	145.14	0.35	—	—	0.92	0.03	—
		0.1791				0.751	0.002	-0.115	146.96	1.86	0.33	4			
		0.1818	70	R	4365	0.739	0.002	—	145.30	0.40	—	—	0.50	0.03	6
		0.1818	70	I	4365	0.736	0.006	—	145.70	0.60	—	—	0.63	0.09	6
		0.1818				0.738	0.004	-0.128	145.50	0.41	-1.13	4			
		0.2362	10	I	<i>81863</i>	0.757	0.003	-0.109	145.77	0.28	-0.87	4	0.25	0.10	2
14139+2906	9174	0.2229	70	I	5263	0.560	0.002	—	91.31	0.30	—	—	0.43	0.04	3
		0.2363	50	I	5374	0.556	0.002	—	91.88	0.28	—	—	0.41	0.38	2
15232+3017	9617	0.4440	70	R	5747	0.549	0.002	0.005	90.38	0.28	-2.39	1	0.39	0.06	9
17571+0004	10912	0.2885	70	R	6710	0.600	0.020	0.080	98.54	0.28	0.13	3	0.37	0.04	7
18096+0400	11111	0.3376	70	R	6800	0.569	0.003	0.009	293.92	0.38	1.23	3	1.41	0.02	8
18208+7120	11311	0.2339	20	I	7180	0.463	0.004	0.035	267.97	0.52	0.93	4	1.33	0.02	1
		0.2365	10	I	7180	0.469	0.003	—	268.29	0.49	—	—	1.35	0.02	2
		0.2366	70	I	7180	0.506	0.005	—	269.31	0.49	—	—	1.30	0.02	2
		0.2366				0.488	0.019	0.059	268.80	0.62	1.76	4	1.33	0.03	
		0.2882	50	R	7180	0.490	0.005	0.061	268.24	0.56	1.23	4	1.42	0.02	7
18339+5221	11468	0.2473	50	R	7123	0.245	0.001	—	117.28	0.34	—	—	0.30	0.04	10
		0.2474	20	R	7123	0.259	0.005	—	116.78	0.57	—	—	0.48	0.11	10
		0.2474				0.252	0.007	0.003	117.03	0.42	-3.48	3	0.39	0.11	
		0.2883	70	V	7028	0.254	0.001	0.005	116.63	0.30	-3.93	3	0.49	0.02	7
22330+6955	16057	0.4193	100	V	8557	0.152	0.009	0.022	152.12	1.86	-0.92	3	1.67	0.12	9
		0.4442	100	R	8557	0.129	0.001	-0.001	142.51	1.27	-10.77	3	0.37	0.14	9

Notes:

- |                                      |                   |  |                   |
|--------------------------------------|-------------------|--|-------------------|
| 1 – foggy, substantial extinction,   | seeing 2.5 arcsec | 6 – very good visibility,              | seeing 3-4 arcsec |
| 2 – foggy, substantial extinction,   | seeing < 2 arcsec | 7 – good visibility,                   | seeing ~ 4 arcsec |
| 3 – good visibility,                 | seeing 2 arcsec   | 8 – variable visibility, some clouds,  | seeing 2.5 arcsec |
| 4 – average visibility, some clouds, | seeing ?          | 9 – average visibility,                | seeing ?          |
| 5 – weak cirrus,                     | seeing ~ 3 arcsec | 10 – variable visibility, some clouds, | seeing ?          |